Electrocatalyst Design

DOI: 10.1002/ange.200501792

Fine Size Control of Platinum on Carbon Nanotubes: From Single Atoms to Clusters**

*Yong-Tae Kim, Kazuyoshi Ohshima, Koichi Higashimine, Tomoya Uruga, Masaki Takata, Hiroyoshi Suematsu, and Tadaoki Mitani**

Electrocatalyst design is a key factor for enhancing the performance of a fuel cell. Since dispersity and cluster size mainly affect the properties of the electrocatalyst, it is necessary to devise a proper synthetic route to highly dispersed and size-controlled clusters.[1,2] Many studies on dispersion and size control of Pt clusters on carbon supports for electrocatalysts have been conducted to investigate the effect of size on electrocatalytic activity from a fundamental scientific viewpoint and to enhance the performance of fuel cells with low noble-metal loadings in engineering applications.[3–11]

Two main chemical routes have been suggested for the preparation of highly dispersed and size-controlled Pt clusters on carbon supports: the colloidal method and impregnation.[12] Several outstanding studies[13–16] have shown that the colloidal method is a successful way to control the size and shape of clusters. However, ligands or protectors should be eliminated from the surface of the resulting electrocatalysts, since the ligands act as surface poisons in electrocatalytic reactions; this process is fairly difficult to perform while still retaining the clusters' size and shape.[17] In contrast, the impregnation method, in which deposition of a precursor is followed by gas- or liquid-phase reduction, is simpler and cheaper than the colloidal method. However, with this method it is quite difficult to control the size and dispersity of clusters on carbon supports, especially those having inert surfaces, since the affinity of the carbon surface for the precursor solution exerts the dominant effect on dispersity in the deposition step.[3]

Herein we suggest a new concept based on a fundamental bottom-up approach to synthesize highly dispersed and size-controlled Pt clusters on carbon supports beyond the limitations of the above two main routes. We call this the single-atom-to-cluster (SAC) approach. It is shown schematically in Scheme 1 and is composed of two steps:

1) Reduction of the Pt precursor $H_2[PtCl_6]$ with $NaBH_4$ on thiolated multiwalled carbon nanotubes (S-MWNTs) to form a monolayer of single Pt atoms (Pt-S-MWNT). The characterization of the single-atom dispersion model is summarized in the Supporting Information.
2) Elimination of the thiol groups by heat treatment at various temperatures T_h followed by slow quenching (q) to room temperature to form Pt clusters ($Pt_{h\text{-}q}$/MWNT) from single atoms.

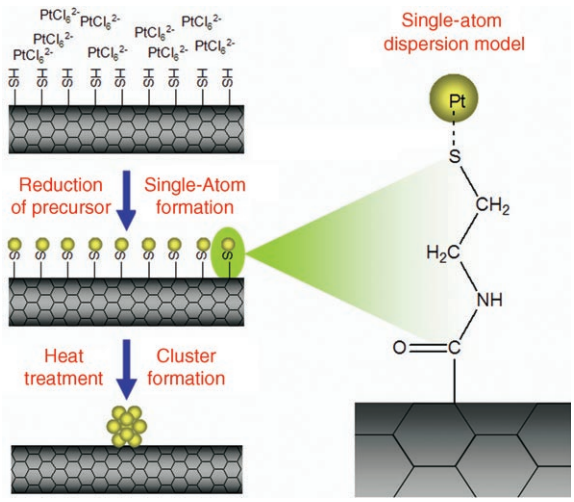

Scheme 1. SAC approach for the formation of size-controlled Pt clusters.

We adopted MWNTs as support for two reasons: First, they have a flat, smooth surface structure without any surface pores that could hinder atoms or clusters from drifting on the surface during the thermal cluster-formation process. Second, MWNTs have superior physicochemical properties as an electrocatalyst support relative to more commonly used carbon black or active carbon.[18–20]

We characterized samples of Pt-S-MWNT, $Pt_{h\text{-}q}$/MWNT (treated at various T_h), and Pt/MWNT prepared by supporting Pt clusters on an untreated MWNT using TEM with an accelerating voltage of 100 kV. The TEM images (Figure 1b–

[*] Y.-T. Kim, K. Ohshima, Prof. T. Mitani
Department of Physical Materials Science
School of Materials Science
Japan Advanced Institute of Science and Technology (JAIST)
1-1 Asahidai, Nomi, Ishikawa 923-1292 (Japan)
Fax: (+81) 761-51-1149
E-mail: mitani@jaist.ac.jp
K. Higashimine
Center for Nano Materials and Technology
Japan Advanced Institute of Science and Technology (JAIST)
1-1 Asahidai, Nomi, Ishikawa 923-1292 (Japan)
Dr. T. Uruga, Dr. M. Takata, Dr. H. Suematsu
Japan Synchrotron Radiation Research Institute (JASRI)/SPring-8
1-1-1 Kouto, Mikazuki, Hyogo 679-5198 (Japan)
Dr. M. Takata
Core Research for Evolutional Science and Technology
Japan Science Technology Cooperation (CREST/JST)
4-1-8 Honcho, Kawaguchi, Saitama 332-0012 (Japan)

[**] This work was partly supported by the Ministry of Education, Science, Sports and Culture of Japan, Grant-in-Aid for Scientific Research (B) No. 17310059 and Nanotechnology Support Project (Proposal No. 2004B0544-ND1b-np-Na/BL02B2, 2005A0701-ND1d-np-Na/BL02B2, 2005A0702-NXa-np/BL01B1) with the approval of Japan Synchrotron Radiation Research Institute (JASRI). We thank Prof. Mikio Miyake for kind help with thermolysis and Dr. Kenichi Kato, Dr. Keiichi Osaka, and Mr. Kazuo Kato for their assistance in measuring XRD and XAFS with synchrotron radiation at SPring-8.

Supporting information for this article is available on the WWW under http://www.angewandte.org or from the author.

f) and size distribution (Figure 1h) of $Pt_{h\text{-}q}$/MWNT at various T_h show that size-controlled clusters are supported on MWNT in $Pt_{h\text{-}q}$/MWNT. However, Pt-S-MWNT has an ambiguous image attributable to dispersed single atoms (Figure 1a). It was possible to observe the disappearance of this ambiguous image and the appearance of clear features with increasing irradiation time by in situ TEM observations with an accelerating voltage of 300 kV (a video clip showing the entire process of cluster formation can be found in the Supporting Information). This phenomenon is due to the formation of clusters through aggregation of single atoms on strong electron-beam irradiation at 300 kV. The clusters in Pt/MWNT (Figure 1g) are considerably larger than in $Pt_{h\text{-}q}$/MWNT and are not uniform, and this reflects the limitations of the impregnation method when using supports with an inert surface.

The structure and electronic state of the size-controlled Pt clusters were characterized by X-ray analysis (Figure 2). The change in crystal structure was confirmed by powder XRD (Figure 2a). Pt-S-MWNT has no peak corresponding to Pt(111) near $2\theta = 27.5°$ ($\lambda = 1.08$ Å), probably because of the dispersed single atoms. However, the sharpening of the XRD patterns of $Pt_{h\text{-}q}$/MWNT with rising T_h can be understood as a narrowing effect due to the increasing cluster size. Moreover, the coexistence of sharp and broad peaks for $Pt_{h\text{-}q}$/MWNT ($T_h = 873$ K) reflects the nonuniform size distribution shown in Figure 1h. Thus, the SAC approach more effectively controls cluster size within a range of a few nanometers.

The electronic state of the size-controlled Pt clusters was investigated X-ray photoelectron spectroscopy (XPS, Figure 2b). The Pt 4f binding energy (BE) in Pt-S-MWNT is significantly shifted (by 2.8 eV) to an energy (BE = 73.0 eV) higher than that of Pt foil (BE = 71.2 eV). This shift is similar to that of Pt 4f from the bulk state to isolated Pt atoms,[21] which was attributable to the final-state effect in the Pt 4f core level.[22] Accordingly, the Pt particles in Pt-S-MWNT can probably be considered to be single Pt atoms. On the other hand, the BE of $Pt_{h\text{-}q}$/MWNT approaches that of the bulk state with rising T_h, which is consistent with growing cluster size.

Since X-ray absorption fine structure (EXAFS) and near edge structure (XANES) measurements are generally quite sensitive to structural changes of materials, as demonstrated by computational modeling,[23] we conducted T_h-dependent XANES and EXAFS measurements on the Pt L_{III} absorption edge. The XANES spectra and the radial distribution function (RDF) of the Fourier-transformed EXAFS spectra are presented in Figure 2c and d, respectively. In accordance with the TEM, XRD, and XPS results, we observed a clear change of structure, from single atom to bulk state, in both measurements with increasing T_h. Especially the clear increase in the peak near 2.8 Å, corresponding to 1NN (first nearest neighbor) Pt–Pt distance, in the RDF of the EXAFS

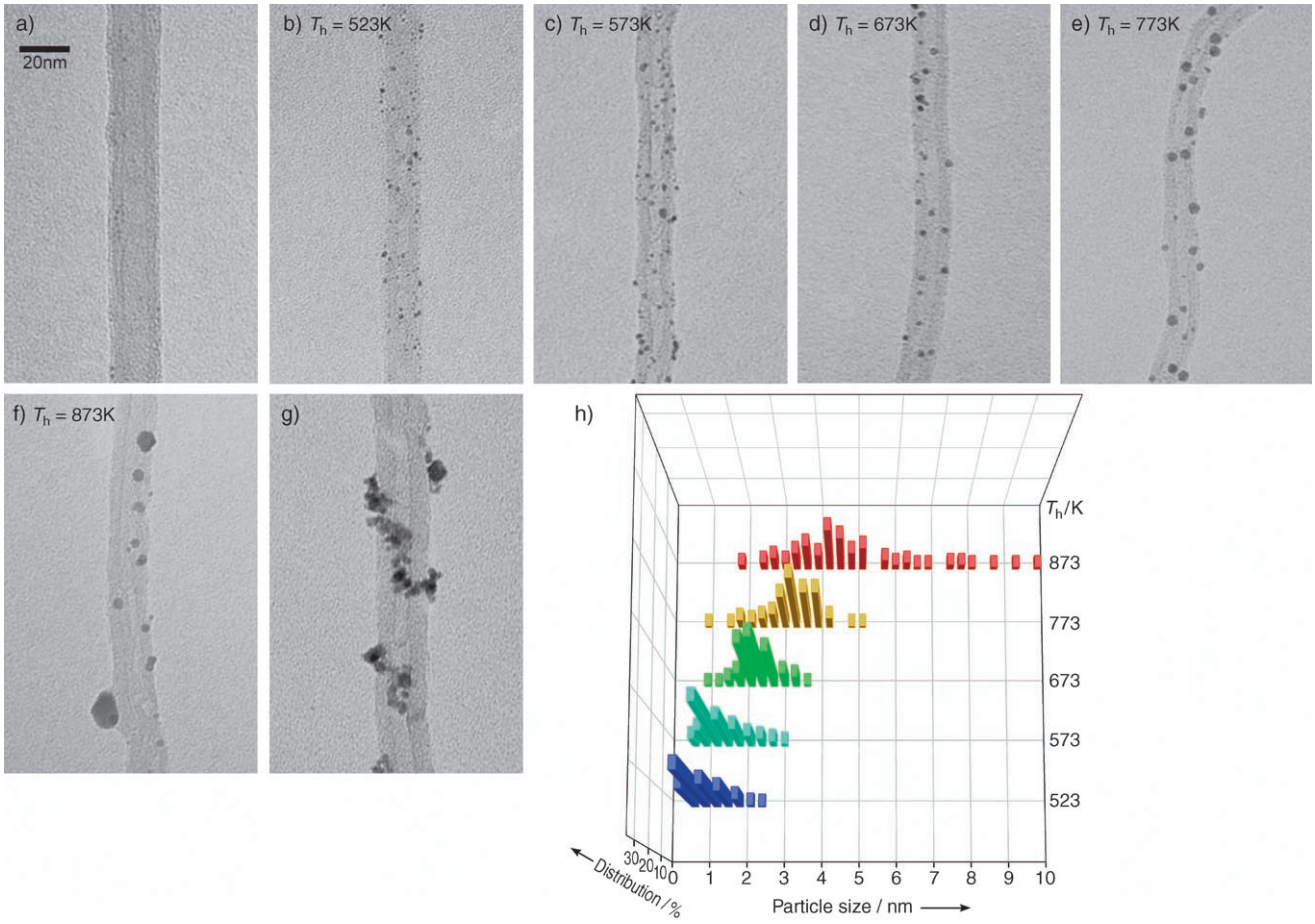

Figure 1. TEM images of a) Pt-S-MWNT, b–f) $Pt_{h\text{-}q}$/MWNT, g) Pt/MWNT; h) size distribution diagram of $Pt_{h\text{-}q}$/MWNT treated at various T_h.

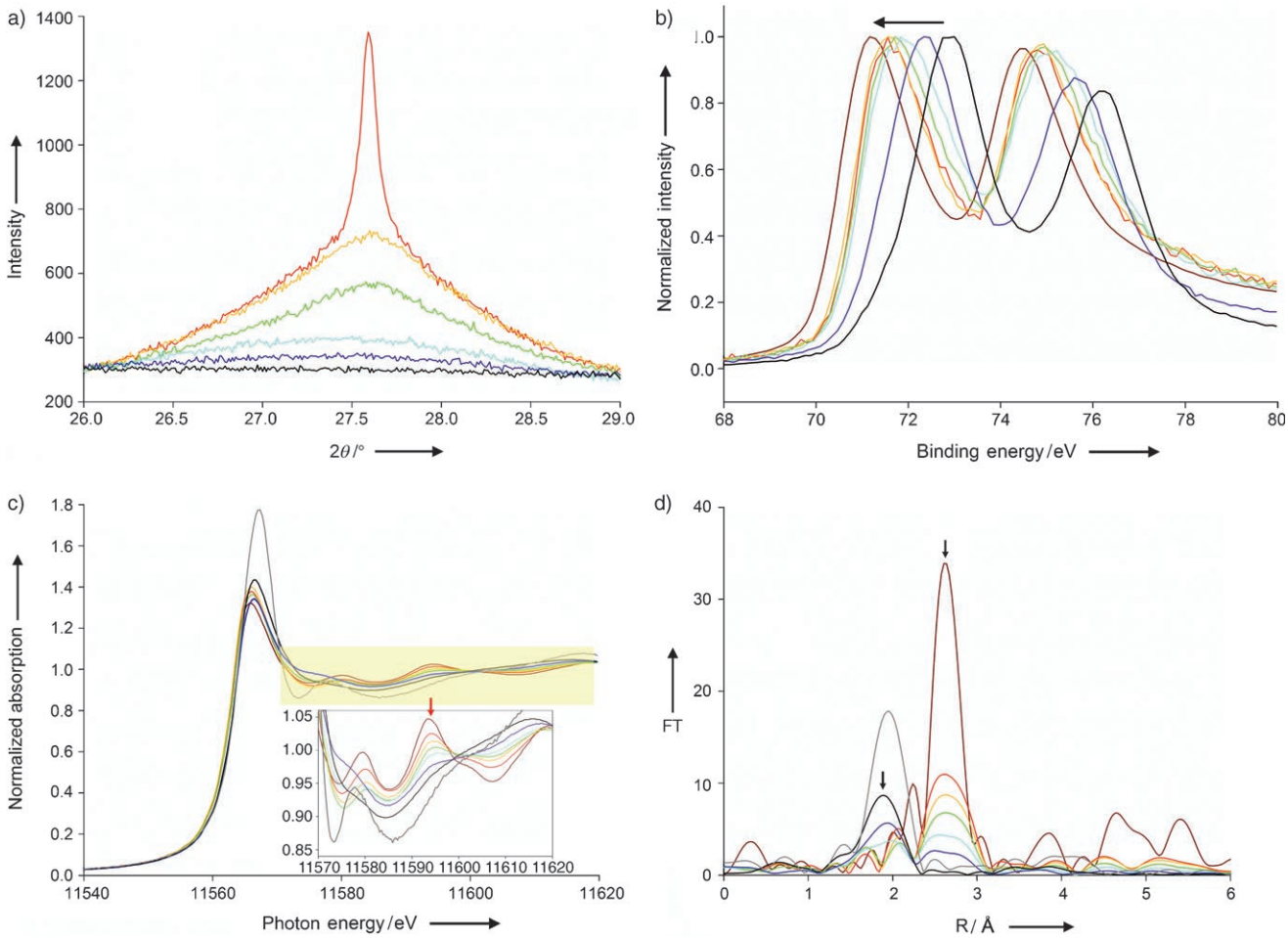

Figure 2. X-ray analyses of Pt-S-MWNT, $Pt_{h\text{-}q}$/MWNT treated at various T_h, and reference materials: $H_2[PtCl_6]$/MWNT as ionic state and Pt foil as bulk state. a) Powder XRD patterns. b) Pt 4f peak shifts of XPS spectra; the arrow indicates the shift of the Pt 4f peak position. c) XANES spectra of Pt L_{III} absorption edge. d) RDF of Fourier-transformed EXAFS spectra; the arrows indicate the peaks corresponding to the Pt–S (around 1.9 Å) and Pt–Pt (around 2.8 Å bonds. —— $H_2[PtCl_6]$/MWNT, —— Pt-S-MWNT, —— $Pt_{h\text{-}q}$/MWNT (T_h = 523 K), —— $Pt_{h\text{-}q}$/MWNT (T_h = 573 K), —— $Pt_{h\text{-}q}$/MWNT (T_h = 673 K), —— $Pt_{h\text{-}q}$/MWNT (T_h = 773 K), —— $Pt_{h\text{-}q}$/MWNT (T_h = 873 K), —— Pt foil.

data (Figure 2d) indicates increasing size with increasing T_h. The EXAFS pattern of Pt-S-MWNT exhibits no peak near 2.8 Å and a strong peak near 1.9 Å for the 1NN Pt–heterogeneous atom distance, that is, only heteroatoms such as the S atom of thiol groups are present around Pt atoms, without any Pt–Pt bonding. Moreover, the valence state of Pt single atoms is considered to be close to that of the bulk state, with a similar height of the white line in the XANES spectra. Accordingly, these results strongly support our single-atom dispersion model.

To investigate the mechanism of the SAC approach to size control we carried out an in situ synchrotron XRD measurement with heat treatment using a large Debye–Scherrer camera which enabled us to observe fine changes of crystal structure with very high speed. Figure 3 shows the in situ XRD patterns and temperature program, respectively. Note that the peak intensity and shape in these in situ measurements do not directly correspond to those of the samples treated at the same T_h in ex situ measurements (Figure 2a), because there are several differences in measurement conditions such as different furnace types, heating rates, atmospheres, and gas flux. As can be seen in Figure 3a, three peaks at each T_h are almost overlapping. This is attributed to the peak-saturation phenomenon after heat treatment for 120 min (raising the temperature for 1 min and waiting for 119 min), which means that the cluster growth stops during or after this waiting process. This phenomenon, which is considered to be a key to understanding the dependence of cluster size on T_h, could be clarified by adopting a well-known concept: the melting point of clusters becomes lower with decreasing size.[24]

According to the Lindemann criterion,[25] the melting point decreases with decreasing cluster size because the larger fraction of surface atoms increases the average atomic displacement. This concept can be described by Equation (1),

$$\frac{T_m(r)}{T_m(\infty)} = \exp\left[-\left(\alpha-1\right)\left(\frac{r}{3h}\right)-1\right]^{-1} \quad (1)$$

derived by Shi,[26] in which r is the cluster radius, α the ratio of mean-square atom displacement on the surface to that inside the cluster, h the height of the atom monolayer in its crystal

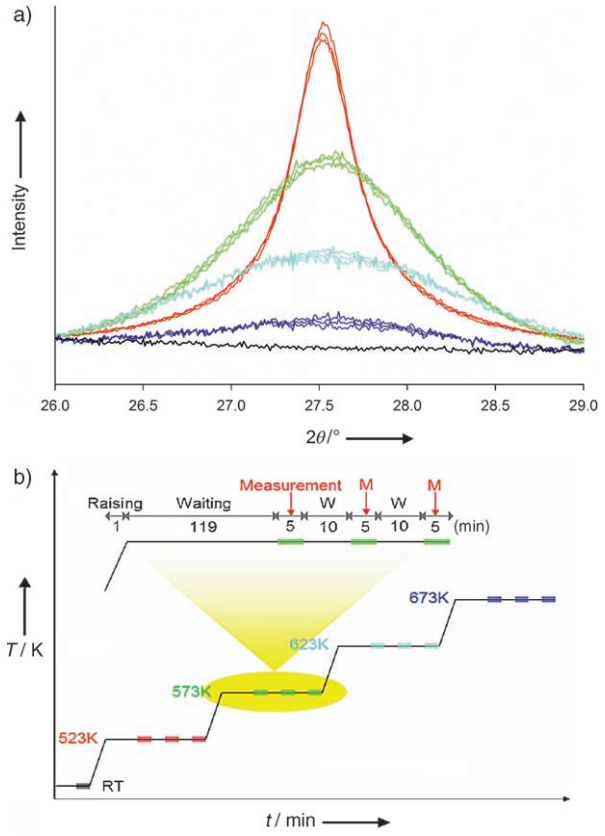

Figure 3. In situ XRD measurements. a) XRD patterns of Pt-S-MWNT as starting material with simultaneous heat treatment. b) Temperature program for in situ XRD measurement. In this program, XRD patterns were recorded three times in a 5-min interval with a 10-min interval in-between at each T_h. Inserting the time interval meant we could more certainly confirm that no more change in the XRD patterns had occurred. —— Pt-S-MWNT, —— $T_h = 523$ K, —— $T_h = 573$ K, —— $T_h = 623$ K, —— $T_h = 673$ K.

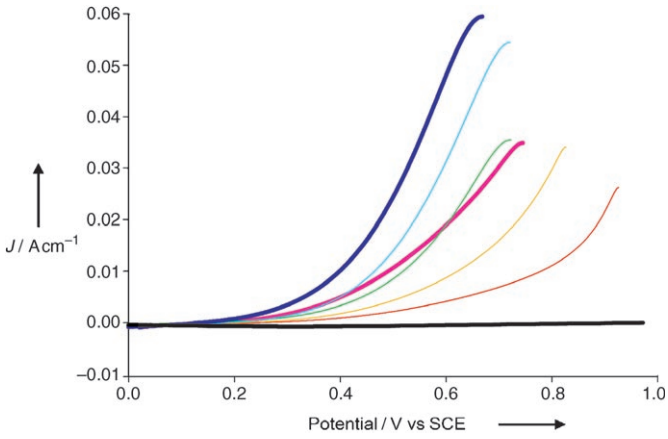

Figure 4. CV patterns for MOR of Pt-S-MWNT and $Pt_{h\text{-}q}$/MWNT treated at various T_h and of Pt/CB. Current densities J are based on the geometric surface area of the working electrode. —— Pt-S-MWNT, —— $Pt_{h\text{-}q}$/MWNT ($T_h = 523$ K), —— $Pt_{h\text{-}q}$/MWNT ($T_h = 573$ K), —— $Pt_{h\text{-}q}$/MWNT ($T_h = 673$ K), —— $Pt_{h\text{-}q}$/MWNT ($T_h = 773$ K), —— $Pt_{h\text{-}q}$/MWNT ($T_h = 873$ K), —— Pt/CB.

structure, and $T_m(r)$ and $T_m(\infty)$ are the melting points in Kelvin of cluster and bulk material, respectively. From Equation (1), it is clear that T_m is dependent on the cluster radius. In other words, when T_m (in this study, T_h) is fixed, the radius (i.e., cluster size) is determined. In our heat treatment, heated clusters (or atoms) drift and meet on a flat MWNT surface that facilitates high drift mobility,[27] and then coincidently melt into larger clusters. After some repetition of this process, growth stops when clusters reach the size having a melting point equivalent to T_h. Hence, this mechanism enables us to control the cluster size by simply setting T_h.

To investigate the electrocatalytic activity of size-controlled clusters in the methanol oxidation reaction (MOR), cyclic voltammetry (CV) was performed with a working electrode coated with prepared samples in 0.5 M H_2SO_4 + 2 M CH_3OH electrolyte with a scan rate of 50 mV s^{-1}. Single Pt atoms of Pt-S-MWNT (black line in Figure 4) have no MOR activity. This result is fairly reasonable, because at least three Pt atoms are required to act as an active site for MOR, according to the model presented in a previous report.[28] Activity appears, however, when Pt clusters are formed by heat treatment. With decreasing cluster size, electrocatalytic activity increases, accompanied by a downward shift in the onset potential, that is, a smaller overpotential for MOR. In comparison to Pt/CB, prepared by supporting Pt clusters on commercial carbon black (Vulcan XC-72), the CV patterns of $Pt_{h\text{-}q}$/MWNT have a sharp threshold, probably due to the superior intrinsic conductivity of MWNTs. We consider that the shift of the onset potential originates from the change of electronic structure, especially the d-band structure of the clusters, induced by increased s–d mixing attributed to the quantum-size effect of the clusters.

In conclusion, we have confirmed the validity and usefulness of the SAC approach to the formation of highly dispersed and size-controlled Pt clusters on MWNTs. The introduction of thiol groups on the MWNT surface resulted in extreme single-atom dispersion, and fine size control of clusters from the dispersed single atoms was achieved by using the concepts of melting-point decrease and high drift mobility on the flat MWNT surface. The introduction of sufficient surface thiol groups is therefore a key factor in the SAC approach. This unique approach is applicable not only to Pt and MWNTs, but also to all kinds of transition metals that form a bond with thiol groups and all kinds of supports or substrates. Furthermore, we believe that this technique can be adapted to all disciplines that require the formation of size-controlled clusters (or of atoms) on supports or substrates, such as catalysts for environmental or fine chemistry, composite electrode materials for lithium secondary batteries and ultracapacitors, as well as electrocatalysts for fuel cells.

Experimental Section

MWNTs prepared by a conventional CVD method were purchased from Helix Material Solutions. Raw soot containing MWNTs was heated for 2 h at 400 °C in static air and subsequently treated with 6 M hydrochloric acid at 70 °C for 12 h. Thiolation of the MWNTs was conducted by a method based on the formation of amide bonds, as

reported previously.[29] Purified MWNTs were stirred in concentrated H_2SO_4/HNO_3 (3/1, 98 and 70% respectively, Kanto Chemical) for 15 min to prepare carboxylated MWNTs, and then chlorinated by refluxing for 12 h with $SOCl_2$ (Wako) at 70°C. After evaporating any remaining $SOCl_2$, thiolated MWNTs (S-MWNTs) were subsequently obtained by reaction with $NH_2(CH_2)_2SH$ (Wako) in dehydrated toluene (Aldrich) for 24 h at 70°C. A suspension of 20 mg of carbon support (MWNT, S-MWNT, or carbon black (CB, Vulcan XC-72)) and 3.125 mL of 10 mM $H_2[PtCl_6]$ (Aldrich), equivalent to 20% weight ratio of Pt to carbon, was prepared by sonication in 40 mL of deionized water. Subsequently, the Pt precursor was simultaneously reduced and supported on the carbon support by using $NaBH_4$ (Kanto chemical) and then washed with deionized water and ethanol several times. After evaporation and drying, we obtained 20% Pt supported on carbon supports, such as MWNT, S-MWNT, and CB, referred to as Pt/MWNT, Pt-S-MWNT, and Pt/CB, respectively. The 20% Pt precursor supported on MWNT ($H_2[PtCl_6]$/MWNT) was prepared by simple evaporation of solvent from a solution of 20 mg of MWNT and 3.125 mL of 10 mM $H_2[PtCl_6]$. Heat treatment of Pt-S-MWNT was performed for 10 min at 523, 573, and 673 K, and for 60 min at 773 and 873 K, in an H_2 gas flow of 100 sccm (standard cubic centimeter per minute). The samples obtained by heat treatment followed by slow quenching of Pt-S-MWNT are denoted by $Pt_{h\text{-}q}$/MWNT (T_h).

The TEM (H-7100 (100 kV) and H-9000NAR (300 kV), Hitachi) images in Figure 1 and those of the in situ measurements in the video clip were obtained with accelerating voltages of 100 and 300 kV, respectively. X-ray diffraction (XRD) analysis was carried out with synchrotron radiation of BL02B2, SPring-8, equipped with a large Debye–Scherrer camera[30] adjusted to a wavelength of 1.08 Å by an Si(111) plane monochromator. In situ XRD patterns were obtained by raising T_h of the H_2-filled sample capillary with the temperature program shown in Figure 3b. XPS (PHI 5600, ULVAC-PHI) was used to confirm the electronic state of Pt clusters and for elemental analysis. The X-ray source was $Al_{K\alpha}$ with an energy of 1486.6 eV operating at 15 kV and 300 W, and the obtained binding energies were referred to C 1s (284.5 eV) of the carbon supports. XANES and EXAFS data for Pt L_{II} and L_{III} absorption edges were obtained in transmission mode with the synchrotron radiation of BL01B1, SPring-8, at room temperature. X-rays were monochromated with two Si(111) plane gratings and detected by two ion chambers, which were continuously purged with a gas mixture of 15% Ar and 85% N_2 in I_0 and 100% Ar gas in I_1. Data reduction was carried out with the computer software REX2000 (Rigaku). The XANES spectrum was normalized by the Victoreen function and the RDF of EXAFS was obtained by a Fourier transform, in the range from 3 to 14 $Å^{-1}$ in k space, on k^3-weighted EXAFS oscillations. The electrocatalytic activity in the MOR was evaluated by CV (608A, ALS). The voltammograms were recorded at a scan rate of 50 $mV s^{-1}$ from −0.24 to 0.96 V (vs SCE) in a 0.5 M H_2SO_4 + 2 M CH_3OH electrolyte after purging with N_2 gas for 1 min and electrochemical cleaning with a fast scan rate. The working electrode was a glassy carbon electrode, 3 mm in diameter, coated with the electrocatalyst layer. Three milligrams of 20% Pt supported on carbon powder and 6 μL of ethanol containing 5 wt% Nafion solution were placed in 150 μL of isopropyl alcohol and suspended with sonication for 1 h. A 6-μL portion of this slurry was dropped onto a glassy carbon electrode and dried in an oven at 60°C for 1 h. The counter- and reference electrodes were a Pt wire and a saturated calomel electrode (SCE), respectively.

Received: May 24, 2005
Revised: September 28, 2005
Published online: December 9, 2005

[1] A. Wieckowski, E. R. Savinova, C. G. Vayenas, *Catalysis and Electrocatalysis at Nanoparticle Surface*, Marcel Dekker, New York, **2003**.
[2] W. Vielstich, A. Lamm, H. Gasteiger, *Handbook of Fuel Cells: Fundamentals, Technology and Applications*, Wiley, New York, **2003**.
[3] K. Kinoshita, P. Stonehart in *Modern Aspects of Electrochemistry* (Eds.: J. O. M. Bockris, B. E. Conway), Plenum, New York, **1977**, p. 12.
[4] M. Watanabe, M. Uchida, S. Motoo, *J. Electroanal. Chem.* **1987**, *229*, 395.
[5] V. H. Bönnemann, W. Brijoux, R. Brinkmann, E. Dinjus, T. Jousen, B. Korall, *Angew. Chem.* **1991**, *103*, 1344; *Angew. Chem. Int. Ed. Engl.* **1991**, *30*, 1312.
[6] M. Min, J. Cho, K. Cho, H. Kim, *Electrochim. Acta* **2000**, *45*, 4211.
[7] T. Hyeon, S. Han, Y.-E. Sung, K.-W. Park, Y.-W. Kim, *Angew. Chem.* **2003**, *115*, 4488; *Angew. Chem. Int. Ed.* **2003**, *42*, 4352.
[8] F. Maillard, M. Martin, F. Gloaguen, J.-M. Leger, *Electrochim. Acta* **2002**, *47*, 3431.
[9] T. Yoshitake, Y. Shimakawa, S. Kuroshima, H. Kimura, T. Ichihashi, Y. Kubo, D. Kasuya, K. Takahashi, F. Kokai, M. Yudasaka, S. Iijima, *Physica B* **2002**, *323*, 124.
[10] X. Sun, R. Li, D. Villers, J. P. Dodelet, S. Desilets, *Chem. Phys. Lett.* **2003**, *379*, 99.
[11] K. Sasaki, J. X. Wang, M. Balasubramanian, J. McBreen, F. Uribe, R. R. Adzic, *Electrochim. Acta* **2004**, *49*, 3873.
[12] A. S. Arico, S. Srinivasan, V. Antonucci, *Fuel Cells* **2001**, *1*, 133.
[13] G. Schmid, *Nanoparticles: From Theory to Application*. Wiley-VCH, Weinheim, **2003**.
[14] R. Wang, J. Yang, Z. Zheng, M. D. Carducci, J. Jiao, S. Seraphin, *Angew. Chem.* **2001**, *113*, 567; *Angew. Chem. Int. Ed.* **2001**, *40*, 549.
[15] V. F. Puntes, K. M. Krishnan, A. P. Alivisatos, *Science* **2001**, *291*, 2115.
[16] Y. Sun, Y. Xia, *Science* **2002**, *298*, 2176.
[17] T. J. Schmidt, M. Noeske, H. A. Gasteiger, R. J. Behm, P. Britz, W. Brijoux, H. Bonnemann, *Langmuir* **1997**, *13*, 2591.
[18] P. Serp, M. Corrias, P. Kalck, *Appl. Catal. A* **2003**, *253*, 337.
[19] G. Che, B. B. Lakshmi, E. R. Fisher, C. R. Martin, *Nature* **1998**, *393*, 346.
[20] S. H. Joo, S. J. Choi, I. Oh, J. Kwak, Z. Liu, O. Terasak, R. Ryoo, *Nature* **2001**, *412*, 169.
[21] W. Eberhardt, P. Fayet, D. M. Cox, Z. Fu, A. Kaldor, R. Sherwood, D. Sondericker, *Phys. Rev. Lett.* **1990**, *64*, 780.
[22] G. K. Wertheim, S. B. DiCenzo, S. E. Youngquist, *Phys. Rev. Lett.* **1983**, *51*, 2310.
[23] A. I. Frenkel, C. W. Hills, R. G. Nuzzo, *J. Phys. Chem. B* **2001**, *105*, 12689.
[24] M. Takagi, *J. Phys. Soc. Jpn.* **1954**, *9*, 359.
[25] F. A. Lindemann, *Phys. Z.* **1910**, *11*, 609.
[26] F. G. Shi, *J. Mater. Res.* **1994**, *9*, 1307.
[27] B. C. Regan, S. Aloni, R. O. Ritchie, U. Dahmen, A. Zettl, *Nature* **2004**, *428*, 924.
[28] B. D. McNichol, *J. Electroanal. Chem.* **1981**, *118*, 71.
[29] J. Liu, A. G. Rinzler, H. Dai, J. H. Hafner, R. K. Bradley, P. J. Boul, A. Lu, T. Iverson, K. Shelimov, C. B. Huffman, F. Rodriguez-Macias, Y.-S. Shon, T. R. Lee, D. T. Colbert, R. E. Smalley, *Science* **1998**, *280*, 1253.
[30] E. Nishibori, M. Takata, K. Kato, M. Sakata, Y. Kubota, S. Aoyagi, Y. Kuroiwa, M. Yamakata, N. Ikeda, *Nucl. Instrum. Methods Phys. Res. Sect. A* **2001**, *467–468*, 1045.

Keywords: carbon · electrocatalysts · electrochemistry · nanotubes · platinum

